

Spin-up problem in superfluid ^4He

P. W. Adams, M. Cieplak,* and W. I. Glaberson

Serin Physics Laboratory, Rutgers University, Piscataway, New Jersey 08854

(Received 21 November 1984)

We report the results of an experimental investigation of the nature of the vortex-boundary interaction and its role in the spin-up problem of superfluid ^4He . We find evidence for two independence vortex-drag mechanisms—a drag associated with vortex lines pulling against pinning sites with a force equal to the line “tension” and a viscous drag associated with vortex motion through the normal-fluid Ekman layers.

I. INTRODUCTION

Probably the most straightforward experimental test of any dynamical model of rotating superfluid helium is the classic spin-up problem in which a freely rotating bucket of superfluid is impulsively spun up and allowed to relax back to solid-body rotation. The transient behavior of the container as it transfers angular momentum to the fluid not only probes the nature of the internal fluid dynamics but also the interaction of the fluid with the walls of the container. It is the latter problem that this paper addresses. Specifically, an experimental study of the nature of the vortex-boundary interaction and its role in the transient behavior of rotating He II is presented.

The investigation of the spin-up problem of He II is not new. In the early seventies Tsakadze and Tsakadze¹⁻³ performed several spin-up experiments, both below and above T_λ , in which they attempted to simulate the “spin-up” behavior observed in some pulsars⁴⁻⁶ (Crab, Vela, etc.) and to characterize superfluid relaxation in general. They observed exponential-like decay in He I and in He II, the major difference between the two being that He II relaxation was slightly quicker. When they roughened the container's inner walls in order to investigate their interaction with the superfluid they observed much shorter relaxation times ($\sim \frac{1}{3}\tau_{\text{smooth}}$), which were independent of temperature through T_λ . This curious result was thought to be a consequence of normal-fluid turbulence.⁷

More recently Campbell and Krasnov⁸ have attempted to explain the results of some early experiments of Reppy and Lane^{9,10} and Reppy *et al.*¹¹ in which He II was spun up from rest. In these experiments it was found that after an initial normal-fluid relaxation the superfluid component induced a relaxation characterized by

$$\Omega_c(t) = A \left[1 - \frac{B}{1+B + Ce^{-t/\tau}} \right]$$

($\Omega_c \equiv$ container angular velocity), qualitatively very different from the typical exponential decay of a classical fluid. Campbell and Krasnov have produced a model of these experiments which incorporates a viscous vortex-boundary interaction in which the vortex-drag force is simply proportional to the relative vortex-surface velocity. By varying the strength of the interaction they were able

to fit the data of Reppy and Lane quite well, giving further evidence to the widely held assumption that a moving vortex line is indeed subject to a viscous force at the fluid-boundary interface. The quality of their model's predictions does not, however, make a compelling case for a viscous interaction. They only considered spin up from rest in which necessarily large fractional changes in vorticity occur. Clearly, in such cases vortex nucleation at the outer walls of the container becomes an important, if not the primary, superfluid relaxation mechanism. Furthermore, as Campbell and Krasnov point out themselves, “. . . there is some difficulty in understanding how the alternate attachment and release (after some stretching) of a vortex line on surface irregularities could result in a dissipative force proportional to the relative velocities.”

A series of rotating counterflow experiments initially performed by Yarmchuck and Glaberson¹² and later continued by Hegde and Glaberson¹³ have provided some tentative evidence that the vortex-boundary interaction is in fact not viscouslike. They indirectly measured the transverse vortex line velocity in a counterflow channel as a function of flow velocity. When measurements were made in “smooth” channels they found a linear dependence upon flow velocity with nearly zero intercept. However, when the channels were roughened they observed that below a certain critical flow velocity the vortices were absolutely pinned and above this critical velocity the dependence was again linear with approximately the same slope as before. Hegde and Glaberson numerically solved the two-fluid hydrodynamic equations for finite-height channel flow and were able to show that the observed critical velocity could be interpreted as that necessary to bring the average vorticity at the surface parallel to the surface.

The present paper reports some recent experimental evidence for a “static-friction” type of vortex-boundary interaction in which the vortices appear to move along a surface exerting a force equal to the vortex-line tension. In Sec. II, this interaction, along with the viscous interaction of Campbell and Krasnov, is incorporated into the standard vortex-line equations for rotating He II. In Sec. III, a description of the experimental apparatus and procedure is given. In Secs. IV and V, the experimental results along with the corresponding numerical solutions to the equations of motion are presented and discussed. Fi-

nally, a low-temperature approximation to the characteristic superfluid relaxation time is derived in the Appendix.

II. EQUATIONS

The equations of motion stated in this section are essentially the same as those used by Campbell and Krasnov, except for the form of the vortex-boundary force. Since the experiments considered consist of spinning up a cylindrical container of He II, the equations are presented in their cylindrically symmetric form. For simplicity, it is assumed that the superfluid velocity has no z dependence and that all equilibration processes are isothermal. Under these conditions the normal-fluid, superfluid, boundary, and vortex line velocities are of the form

$$\begin{aligned}\bar{V}_n &= (0, V_{n\phi}, 0), \\ \bar{V}_s &= (0, V_{s\phi}, 0), \\ \bar{V}_b &= (0, r\Omega_c, 0), \\ \bar{V}_L &= (V_{Lr}, V_{L\phi}, 0),\end{aligned}\quad (1)$$

and satisfy

$$\frac{\partial \bar{V}_L}{\partial \phi} = \frac{\partial \bar{V}_n}{\partial \phi} = \frac{\partial \bar{V}_s}{\partial \phi} = \frac{\partial \bar{V}_b}{\partial \phi} = 0, \quad (2)$$

$$\frac{\partial \bar{V}_s}{\partial z} = \frac{\partial \bar{V}_L}{\partial z} = 0.$$

The superfluid velocity is given by

$$V_{s\phi}(r) = \frac{\Gamma}{r} \int_0^r r' n(r', t) dr', \quad (3)$$

where $n(r, t)$ is the vortex-line density and $\Gamma \equiv h/m_{\text{He}}$. Conservation of vorticity requires that $n(r, t)$ satisfy

$$\frac{\partial n}{\partial t} = -\frac{1}{r} \frac{\partial}{\partial r} (rnV_{Lr}). \quad (4)$$

The normal-fluid relaxation is governed by the usual Navier-Stokes equation along with an additional vortex-drag term,

$$\begin{aligned}\rho_n \frac{\partial V_{n\phi}}{\partial t} &= \eta \left[\frac{\partial^2 V_{n\phi}}{r^2} + \frac{1}{r} \frac{\partial V_{n\phi}}{\partial r} - \frac{V_{n\phi}}{r^2} + \frac{\partial^2 V_{n\phi}}{\partial z^2} \right] \\ &\quad - n(r, t) (\bar{F}_n)_{\hat{\phi}},\end{aligned}\quad (5)$$

where η is the normal-fluid viscosity.

Finally, the acceleration of the container is obtained by summing the internal superfluid and normal-fluid torques,

$$\begin{aligned}I_c \dot{\Omega}_c(t) &= 2\pi R \eta \int_{-L/2}^{L/2} \left[V_{n\phi} - r \frac{\partial V_{n\phi}}{\partial r} \right] \Bigg|_R dz \\ &\quad - 4\pi \eta \int_0^R r^2 \left[\frac{\partial V_{n\phi}}{\partial z} \right] \Bigg|_{z=L/2} dr \\ &\quad + 2\pi L \int_0^R n(r, t) r^2 (-\bar{F}_b)_{\hat{\phi}} dr,\end{aligned}\quad (6)$$

where R , L , and I_c are the container's radius, height, and moment of inertia, respectively. The last term represents the superfluid torque arising from the vortex-boundary interaction, where $-\bar{F}_b$ is the force per unit length applied by a vortex line to the top and bottom of the container.

Equations (3)–(6) are complete once \bar{V}_L is related to \bar{V}_s , \bar{V}_n , and \bar{V}_b . Following Hall,¹⁴ \bar{V}_L is determined by requiring that all the forces acting on a given vortex line sum to zero. These forces include the superfluid force (Magnus force) given by

$$\bar{F}_m = \rho_s \bar{\Gamma} \times (\bar{V}_L - \bar{V}_s), \quad (7)$$

where $\bar{\Gamma} = \Gamma \hat{z}$ is the vortex-line circulation, the normal-fluid friction force,

$$\bar{F}_n = -\gamma_0 (\bar{V}_L - \bar{V}_n) - \gamma'_0 \hat{\Gamma} \times (\bar{V}_L - \bar{V}_n), \quad (8)$$

where γ_0 and γ'_0 are phenomenological constants arising from roton scattering cross sections, and the vortex-boundary force which is taken to be the sum of a "static" and a viscous boundary force,

$$\bar{F}_b = \begin{cases} -(\bar{F}_n + \bar{F}_m) |_{\bar{V}_L = \bar{V}_b} & \text{for } |\bar{F}_n + \bar{F}_m| < f_p, \\ -f_p (\hat{V}_L - \hat{V}_b) - \xi \rho_s \Gamma (\bar{V}_L - \bar{V}_b) & \text{for } |\bar{F}_n + \bar{F}_m| > f_p, \end{cases} \quad (9)$$

where f_p is the minimum force per unit length required to break loose a pinned vortex, and ξ is the dimensionless viscous interaction strength. Though f_p and ξ are treated as adjustable parameters, $f_p L$ is assumed to be of the order

$$T_L = \frac{\rho_s \Gamma^2}{4\pi} \ln \left[\frac{b}{a} \right], \quad (10)$$

where T_L is the line "tension" of an isolated vortex, a is the vortex-core parameter, and b is the intervortex line spacing.

Splitting the vortex-force equation,

$$\bar{F}_n + \bar{F}_m + \bar{F}_b = 0, \quad (11)$$

into components, we obtain two independent nonlinear equations and two unknowns (V_{Lr} , $V_{L\phi}$), for \hat{r} :

$$\begin{aligned}-\rho_s \Gamma (V_{L\phi} - V_{s\phi}) + \gamma'_0 (V_{L\phi} - V_{n\phi}) - \gamma_0 V_{Lr} \\ - \frac{f_p V_{Lr}}{[V_{Lr}^2 + (V_{L\phi} - r\Omega_c)^2]^{1/2}} - \xi \rho_s \Gamma V_{Lr} = 0,\end{aligned}\quad (12)$$

and for $\hat{\phi}$:

$$\begin{aligned}(\rho_s \Gamma - \gamma'_0) V_{Lr} + \gamma_0 (V_{n\phi} - V_{L\phi}) \\ - \frac{f_p (V_{L\phi} - r\Omega_c)}{[V_{Lr}^2 + (V_{L\phi} - r\Omega_c)^2]^{1/2}} - \xi \rho_s \Gamma (V_{L\phi} - r\Omega_c) = 0.\end{aligned}\quad (13)$$

In principle V_{Lr} and $V_{L\phi}$ can be determined from the above two equations and then substituted into Eqs. (3)–(6) in order to find a solution subject to the following boundary conditions,¹⁵

$$V_{n\phi}(R,z) = R\Omega_c,$$

$$V_{n\phi}(r, \pm L/2) = r\Omega_c. \quad (14)$$

III. APPARATUS

A schematic diagram of the experimental apparatus is shown in Fig. 1(a). The helium cell consisted of a hollow lead-coated magnesium cylinder, *A*, 5 cm high and 2.8 cm in radius. The cylinder contained a set of thin aluminum disks and spacers which formed eight cylindrical cells, *B*, each with a typical height to radius ratio of 0.21. The cylinder was sealed with a magnesium cap into which a small hole had been drilled, thus minimizing film flow out of the container during a run. After submerging the container in He II for a time sufficient to fill through the cap hole, the inner jar, *C*, was emptied via a fountain pump, *D*.

The container was levitated via a superconducting magnet, *E*, surrounding its base. Axial stability was provided by a second superconducting magnet, *F*, positioned over the top portion of the container.

Once levitated, the container was accelerated by a non-contacting induction motor consisting of a thin copper sleeve, *G*, surrounded by four superconducting drive coils, *H*. Typical maximum angular accelerations were on the order of 0.15 rad/s^2 . The induction motor drive was provided by a computer-controlled Wavetek waveform synthesizer which allowed precise control of the spin-up torque's magnitude and duration. Computer control of the drive was also useful in nulling external drag since

rotation-dependent compensation torques could easily be produced. The angular velocity of the container was measured by a dual photodetection system, *I*, and a computer (Omnibyte OB68K) monitored clock.

IV. EXPERIMENTAL RESULTS

The experimental procedure involved impulsively spinning up (and spinning down) the container of He II from $\Omega_c = \omega_0$ to $\Omega_c = \omega_1 = \omega_0 + \Delta\omega$. The container's angular velocity $\Omega_c(t)$, was then monitored as a function of time. The experiments were performed at $T = 2.1$ and 1.3 K with both smooth disks and roughened disks, coated with No. 320 aluminum-oxide powder.

Shown in Fig. 2 is the response of the container when empty. As expected, since there was no source of internal torques, no transient behavior was observed. It should be pointed out that the line in Fig. 2, as with all of the decay curves presented in this section, is actually the average response of many (~ 20) computer controlled repetitions of the same experiment. This signal averaging technique enabled us to produce signal-to-noise ratios that were unobtainable in a single sweep.

For the helium-filled cell, the character of the $T = 1.3$ K relaxations depended dramatically on the disk surface roughness. Figure 3 shows a typical response of the smooth-surfaced cell to an impulsive torque and Figs. 4 and 5 are typical responses for the rough-surfaced cell. Note the exponential-like behavior of the former and the nearly linear response of the latter. Substantial departure from exponential-like behavior was characteristic of all the low-temperature rough-disk relaxations for which $\omega_0 > 1.5 \text{ rad/s}$. The remarkable linearity of these decay curves, observed to be symmetric with respect to spin up and spin down, indicates that the superfluid applied a strong, relatively constant, internal torque throughout most of the relaxation. In light of our model, we attribute the source of this torque to a "frictional" type of force resulting from the alternate pinning and depinning of vortices as they move across surface protuberances during the superfluid relaxation. The magnitude of this force is

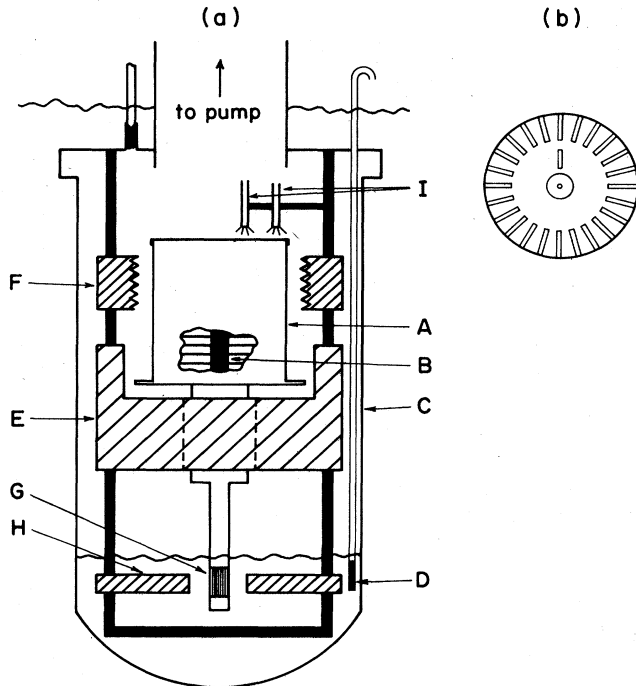


FIG. 1. (a) Schematic diagram of the experimental apparatus. (b) Arrangement of photodetector marks on the top of the cell.

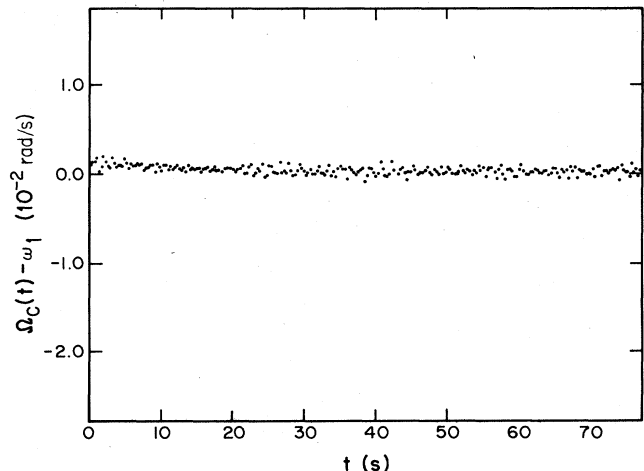


FIG. 2. Response of the cell when empty, following an impulsive torque ($\omega_0 = 2.36 \text{ rad/s}$, $\Delta\omega = 0.283 \text{ rad/s}$).

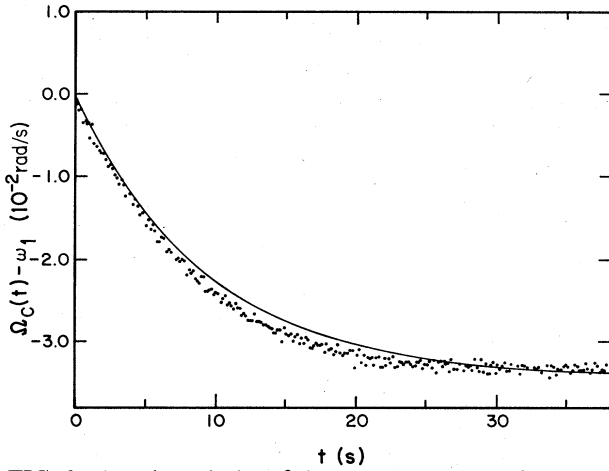


FIG. 3. Angular velocity of the smooth-disk cell after an impulsive spin-up torque ($\omega_0=8.54$ rad/s, $\Delta\omega=0.283$ rad/s, $T=1.3$ K). The solid line represents the prediction of our model for $\xi=0.005$ and $f_p=0.0$.

represented by the “static” interaction parameter, f_p .

Simulations of the experiments were made in which ξ and f_p were independently adjusted to fit the low-temperature data. The exponential-like behavior of the smooth-disk data suggests that viscous drag was the dominant superfluid-container interaction. The smooth disk decays were therefore fit by setting $f_p=0$ and varying ξ . This is equivalent to the approach taken by Campbell and Krasnov. The numerical fit is shown in Fig. 3 as the solid line. The slight linearity of the data is probably a consequence of not having perfectly smooth disks. Reasonable fits were obtained with ξ ranging from 0.005 to 0.007 for all of the smooth-disk data, ξ increasing with decreasing rotation speed. As discussed in the next section, these values of ξ are consistent with treating the drag as arising

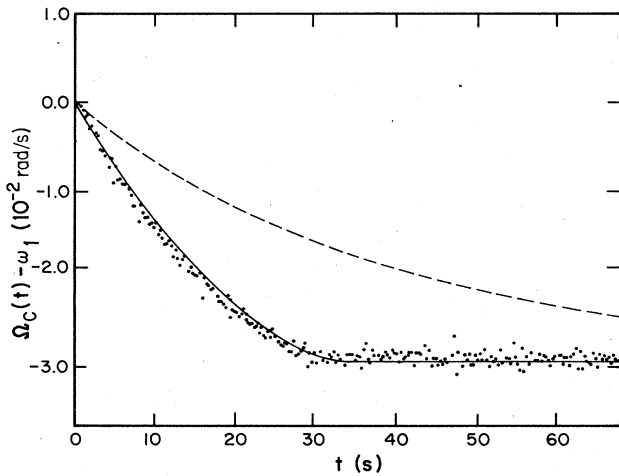


FIG. 4. Angular velocity of the rough-disk cell after an impulsive spin-up torque ($\omega_0=2.21$ rad/s, $\Delta\omega=0.283$ rad/s, $T=1.3$ K). The solid curve is the prediction for $\xi=0.005$ and $f_p=0.53 \times 10^{-6}$ dynes/cm. The dashed curve is the prediction for $\xi=0.005$ and $f_p=0.0$.

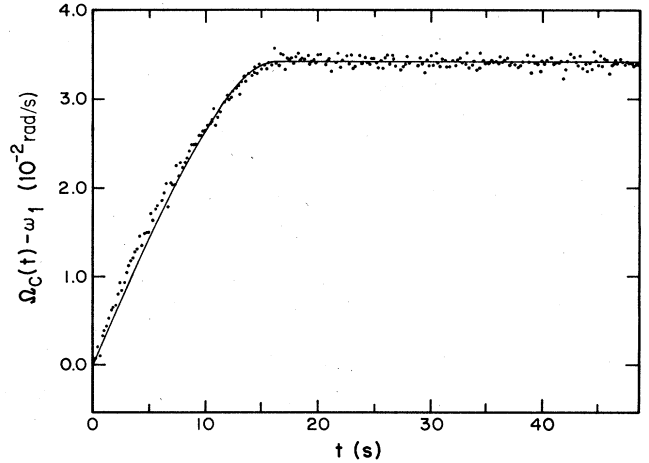


FIG. 5. Angular velocity of the rough-disk cell after an impulsive spin-down torque ($\omega_0=3.35$ rad/s, $\Delta\omega=-0.283$ rad/s, $T=1.3$ K). The solid curve is the prediction for $\xi=0.005$ and $f_p=0.53 \times 10^{-6}$ dynes/cm.

from mutual friction in the Ekman layer.

The rough-disk relaxations were fit by simply “turning on” the static interaction. It was assumed that ξ was independent of surface roughness, thus leaving f_p as the only adjustable parameter. Excellent fits to all of the rough-disk data for which $\omega_0 > 1.5$ rad/s, were obtained with $f_p=0.53 \times 10^{-6}$ dynes/cm and were relatively insensitive to the values of ξ . Examples of such fits are shown as the solid lines in Figs. 4 and 5. This value of f_p corresponds to a maximum line “tension,” assuming a vortex line cannot apply a force to the boundary greater than its tension, of

$$T_L \approx \frac{1}{2} L f_p = 1.59 \times 10^{-7} \text{ dynes}, \quad (15)$$

in good agreement with the expected value,

$$T_L = \frac{\rho_s \Gamma^2}{4\pi} \ln \left[\frac{b}{a} \right] = 1.5 \times 10^{-7} \text{ dynes}. \quad (16)$$

Note that the approach we have taken suggests that observation of the spin-up rate of the superfluid yields a reasonably direct measure of the quantum of circulation (see Appendix).

At $T=2.1$ K, where $\rho_n/\rho=0.88$, we observed exponential-like behavior that was independent of disk roughness. Simulations of these relaxations yielded poor results—predicting decay times much longer than what was observed. It seems likely that the poor quality of our fits at these higher temperatures was due to normal-fluid secondary flow.

V. DISCUSSION AND CONCLUSION

The lowest temperature we were able to investigate was 1.3 K. This in conjunction with the fact that the normal-fluid components of our equations are incomplete, prevented us from realistically investigating the temperature dependence of ξ and f_p . In principle, the complete

Navier-Stokes equation could have been included in the equations of motion, thus enabling us to perform simulations at higher temperatures. This, however, would have presented formidable numerical difficulties beyond the scope of this investigation. Nevertheless, inferences can be made about the temperature dependence of the interaction parameters.

In our model of pinning, a vortex line is absolutely immobilized on a surface protuberance until external forces stretch it to the point where it bends parallel to the surface at the surface. At this depinning threshold the vortex line can apply a maximum force, antiparallel to the sum of the forces acting upon it, equal to its energy per unit length. Thus, f_p has a well-defined theoretical value,

$$f_p = \frac{2T_L}{L}, \quad (17)$$

which scales with temperature as ρ_s . An experimental verification of this temperature dependence is needed to guarantee that the agreement between simulation and theory was not fortuitous.

The case for ξ is not clear since it is not understood how a vortex line can apply a viscous force to the boundary. In fact, it is aesthetically displeasing that a boundary interaction of unknown origin had to be included into the model in order to fit all of the data. Though the rough-disk data could be fit reasonably well with $\xi=0$ and $f_p=0.75 \times 10^{-6}$ dynes/cm, we were unable to obtain the exponential character of the smooth-disk relaxations. Furthermore, the value of f_p determined with $\xi=0$ was somewhat too large considering our model of pinning.

A possible explanation for the necessity of including a viscous interaction in our model, lies in the aforementioned inadequacy of the normal-fluid equations. By neglecting the axial and radial components of the normal fluid velocity we have implicitly assumed that the normal fluid relaxes via viscous diffusion. However, it is well known that secondary flow is the primary relaxation mechanism in all contained (Newtonian) spin-up flows.¹⁶ Secondary flow is characterized by a quasisteady Ekman layer at each disk surface through which fluid is pumped radially by centrifugal action. We believe it is this viscous layer, unaccounted for in the simulations, that requires the *ad hoc* addition of a viscous vortex-boundary interaction to our model.

For a typical $T=1.3$ K spin-up experiment in which $\omega_0=3$ rad/s, $\eta=16 \times 10^{-6}$ P, and $\rho_n=0.007$ g/cm³, the thickness of the Ekman layer on each disk is

$$d_E \simeq \left[\frac{\eta}{\rho_n \omega_0} \right]^{1/2} \simeq 0.03 \text{ cm}. \quad (18)$$

The total normal-fluid friction force on a vortex line due to its motion through the top and bottom Ekman layers (assuming that in the layers $\bar{V}_n \simeq \bar{V}_b$) is

$$\bar{F}_E = 2(d_E)\gamma_0(\bar{V}_L - \bar{V}_b). \quad (19)$$

After equating \bar{F}_E to the viscous interaction of our model and solving for ξ , we obtain

$$\xi = \frac{2d_E\gamma_0}{L\rho_s\Gamma} \simeq 3.3 \times 10^{-3}, \quad (20)$$

a value surprisingly close to that used in the simulations. Equation (20) is also qualitatively consistent with the observed ω_0 dependence of ξ . This lends strong evidence to our suspicions that the viscous part of our vortex-boundary interaction is associated with the mutual friction exerted by the vortices moving through the Ekman layers.

At low temperatures, the normal-fluid friction parameter γ_0 is approximated by

$$\gamma_0 \simeq \frac{\rho_s \rho_n \Gamma B}{2\rho} \quad (B \sim 1.5), \quad (21)$$

which, when plugged into the expression for ξ , gives

$$\xi \simeq \frac{B}{\rho L} \left[\frac{\rho_n \eta}{\omega_0} \right]^{1/2}. \quad (22)$$

If ξ does indeed represent vortex drag through normal-fluid Ekman layers, it should scale with temperature as $\rho_n^{1/2}$ at low temperatures.

As a final note, the value of ξ used to fit our data is four orders of magnitude smaller than typical values used by Campbell and Krasnov. It can easily be shown (see Appendix) that at low temperatures the smooth-disk ($f_p=0$) relaxation time τ_s is proportional to $(\xi^2 + 1)/\xi$, so that $\tau_s(\xi=0.005) \simeq \tau_s(\xi=200)$. Although the smooth data could be fit with either $\xi=0.005$ or $\xi=200$, the rough data restricted ξ to small values.

ACKNOWLEDGMENT

This work was supported in part by the National Science Foundation.

APPENDIX

The hydrodynamic equations of Sec. II are greatly simplified in the low-temperature limit where their normal-fluid components can be neglected ($\rho_n = \gamma_0 = \gamma'_0 = 0$). Under this simplification, a relaxation time τ can be derived for two separate cases. The first corresponds to the rough-disk relaxations which we assume to be dominated by the "static" vortex-boundary interaction so that ξ can be set to zero. In the second case f_p will be set to zero and τ will be derived in terms of ξ . This last derivation closely follows that of Campbell and Krasnov.

After setting $\xi=0$ and neglecting the normal fluid, analytic expressions for V_{Lr} and $V_{L\phi}$ are easily obtained from Eqs. (12) and (13),

$$V_{Lr}(r) = \pm \gamma \left[1 - \frac{\gamma^2}{B^2} \right]^{1/2}, \quad (A1)$$

$$V_L(r) = B \left[1 - \frac{\gamma^2}{B^2} \right] + r\Omega_c, \quad (A2)$$

where

$$\gamma \equiv \frac{f_p}{\rho_s \Gamma},$$

and

$$B \equiv V_{s\phi}(r) - r\Omega_c.$$

Using (A1) in Eq. (6), we have

$$I_c \dot{\Omega}_c = -2\pi L \int_{r_0}^R r^2 n(r) f_p \left[1 - \frac{\gamma^2}{B^2} \right]^{1/2} dr. \quad (\text{A3})$$

If we now consider a specific experiment in which the container is impulsively spun up from angular velocity ω_0 to angular velocity ω_1 , then the minimum radius r_0 , at which vortices will be unpinned by the Magnus force, is given by

$$\rho_s \Gamma [V_{s\phi}(r_0) - \Omega_c r_0] + f_p = 0.$$

Since

$$V_{s\phi}(r_0) - \Omega_c r_0 = r_0(\omega_0 - \omega_1) = -r_0 \Delta\omega,$$

we find that

$$r_0 = \frac{f_p}{\rho_s \Gamma \Delta\omega}.$$

Assuming $\Delta\omega \ll \omega_0$, $r_0/R \ll 1$, and that the superfluid relaxation is approximately uniform, we can replace $n(r, t)$ by

$$n_0 = \frac{2\omega_0}{\Gamma},$$

and $B(r, t)$ by

$$B_0 = r \Delta\omega(t),$$

in the integrand of Eq. (7),

$$\begin{aligned} I_c \dot{\Omega}_c &\simeq -2\pi L \int_0^R r^2 n_0 f_p \left[1 - \frac{\gamma^2}{B_0^2} \right]^{1/2} dr \\ &\simeq -\frac{2\pi L n_0 f_p R^3}{3} \left[1 + O \left[\frac{\gamma}{R \Delta\omega(t)} \right]^2 \right]. \end{aligned} \quad (\text{A4})$$

Equation (A4) remains a valid approximation to the relaxation as long as the outer vorticity which dominates the torque in (A3) remains strongly unpinned. For $f_p \sim 10^{-6}$ dynes/cm and $r_0 \simeq 1$ cm, the relative superfluid-container angular velocity at which repinning begins is

$$\Delta\omega = \frac{f_p}{\rho_s \Gamma r_0} \simeq 10^{-2} \text{ rad/s},$$

indicating that vorticity does not repin until the relaxation

is nearly complete. Assuming that unpinned outer vorticity dominates (A3) throughout virtually all of the relaxation, we find that the solution to (A4) leads to linear decay,

$$\Omega_c(t) = -\frac{2\pi f_p L R^3 n_0}{3I_c} t + \omega_1 = -\frac{4\pi f_p L R^3 \omega_0}{3I_c \Gamma} t + \omega_1. \quad (\text{A5})$$

The final angular velocity of the container is obtained by conservation of momentum,

$$I_c \omega_1 + I_{\text{He}} \omega_0 = (I_c + I_{\text{He}}) \omega_f, \quad (\text{A6})$$

$$\omega_f = \frac{I_c \omega_1 + I_{\text{He}} \omega_0}{I_c + I_{\text{He}}}.$$

If we define the relaxation time τ as the time for the container to decay from ω_1 to $(\omega_1 + \omega_f)/2$, then

$$\Omega_c(\tau) = \frac{\omega_1 + \omega_f}{2} = -\frac{4\pi f_p L R^3 \omega_0}{3I_c \Gamma} \tau + \omega_1 \quad (\text{A7})$$

and

$$\tau = \left[\frac{I_c}{I_c + I_{\text{He}}} \right] \frac{3\Gamma \rho_s R}{16f_p} \frac{\Delta\omega}{\omega_0}. \quad (\text{A8})$$

Replacing f_p by its theoretical value $2T_L/L$, we obtain a simple expression relating the relaxation time to the physical dimensions of the system,

$$\tau = \frac{3\pi R L}{8\Gamma \ln(b/a)} \left[\frac{I_c}{I_c + I_{\text{He}}} \right] \frac{\Delta\omega}{\omega_0}. \quad (\text{A9})$$

Similarly, Eqs. (12) and (13) can be solved for the case where $f_p = 0$ and $\xi \neq 0$,

$$V_{Lr}(r) = \frac{\xi}{1 + \xi^2} B, \quad (\text{A10})$$

$$V_{L\phi}(r) = \frac{V_{s\phi} + \xi^2 r \Omega_c}{\xi^2 + 1}. \quad (\text{A11})$$

As before, using (A11) in (4) and replacing $n(r, t)$ by $n_0 = 2\omega_0/\Gamma$ and then solving the resulting linear first-order differential equation, we find

$$\Omega_c(t) = \omega_f + e^{-t/\tau_s} (\omega_1 - \omega_f), \quad (\text{A12})$$

where

$$\tau_s = \left[\frac{I_c}{I_c + I_{\text{He}}} \right] \frac{\ln(2)}{2\omega_0} \left[\frac{1 + \xi^2}{\xi} \right]. \quad (\text{A13})$$

*Present address: Institute of Physics, Polish Academy of Sciences, Al. Lotnikow 32/46, 02668 Warsaw, Poland.

¹J. S. Tsakadze and S. J. Tsakadze, Phys. Lett. **41A**, 197 (1972).

²J. S. Tsakadze and S. J. Tsakadze, Zh. Eksp. Teor. Fiz. **64**, 1816 (1973) [Sov. Phys.—JETP **37**, 918 (1973)].

³J. S. Tsakadze and S. J. Tsakadze, Usp. Phys. Nauk **115**, 503 (1975) [Sov. Phys.—Usp. **18**, 242 (1975)].

⁴G. S. Downs, J. Appl. Phys. **249**, 687 (1981).

⁵P. R. Backus, J. H. Taylor, and M. Damashek, J. Appl. Phys.

Lett. **225**, L63 (1982).

⁶E. Lohsen, Astron. Astrophys. Suppl. **44**, 1 (1981).

⁷M. A. Alpar, J. Low Temp. Phys. **31**, 803 (1978).

⁸L. J. Campbell and Ya. K. Krasnov, J. Low Temp. Phys. **49**, 377 (1982).

⁹J. D. Reppy and C. T. Lane, in *Proceedings of the VII International Conference on Low Temperature Physics*, edited by G. M. Graham and A. C. H. Hallet (University of Toronto Press, Toronto, 1961), p. 443.

¹⁰J. D. Reppy and C. T. Lane, Phys. Rev. **140**, A106 (1965).

¹¹J. D. Reppy, D. Depatie, and C. T. Lane, Phys. Rev. Lett. **5**, 541 (1960).

¹²E. J. Yarmchuk and W. I. Glaberson, J. Low Temp. Phys. **36**, 381 (1979).

¹³S. G. Hegde and W. I. Glaberson, Phys. Rev. Lett. **45**, 190 (1980).

¹⁴H. E. Hall, Proc. R. Soc. London Ser. A **245**, 546 (1958).

¹⁵We also assume the validity of the equation of continuity, (4), at the boundary $r=R$. This implies unrestricted vortex nucleation and that the vortex density is continuous at the boundary.

¹⁶H. P. Greenspan, *The Theory of Rotating Fluids* (Cambridge University Press, Cambridge, 1968), Chap. 2.